Alteration of Gene Expression in Reactive Astrocytes Induced by Aβ1-42 Using Low Dose of Methamphetamine

Bita Soltanian
Islamic Azad University
marzieh dehghan shasaltaneh (dehghan@znu.ac.ir)
University of Zanjan https://orcid.org/0000-0002-1425-7347
Gholam Hossein Riazi
Tehran University: University of Tehran
Nahid Masoudian
Islamic Azad University

Research Article

Keywords: Alzheimer's disease, Apoptosis, Hyperphosphorylated tau, Methamphetamine

Posted Date: May 17th, 2021

DOI: https://doi.org/10.21203/rs.3.rs-474878/v1

Version of Record: A version of this preprint was published at Molecular Biology Reports on August 10th, 2021. See the published version at https://doi.org/10.1007/s11033-021-06629-x.

Abstract

Background: Alzheimer's disease (AD) is considered as a degenerative brain disorder. Since functional loss of astrocytes is associated with AD, therefore, we investigated the effects of low dose of methamphetamine (METH) on primary fetal human astrocytes under a stress paradigm as a possible model for AD.

Methods and Results: Our assessed groups include Aβ (Group 1), METH (Group 2), Ab + METH (METH after adding Aβ for 24 h: Treated group; Group 3), METH + Ab (Aβ after adding METH for 24 h: Prevention group; Group 4), and control group. The gene expression of *Bax, Bcl-X, PKCa*, *GSK3β,* and *Cdk5* was evaluated. Phosphorylated tau, p-GSK3β, GSK3β, and GSK3α proteins were assessed by western blotting. Cell cycle arrest and apoptosis were checked by flow cytometry and Hoechst staining. The expression of *GSK3β, Cdk5,* and *PKCa* genes decreased in the prevention group, while *GSK3β* and *Cdk5* were amplified in the treatment group. The level of GSK3α and GSK3β proteins in the treatment group increased, while it decreased in the prevention group. A decrease occurred in the percentage of necrosis and early apoptosis in the treatment and prevention groups. The results of cell cycle indicated that G1 increased, while G2 decreased in the prevention group.

Conclusions: The pure form of METH can prevent from activating GSK-3β and CDK-5, as well as enhanced activity of PKCa to inhibit phosphorylated tau protein. Therefore a low dose of METH may have a protective effect or reducing role in the pathway of tau production in reactive astrocytes.

Introduction

Alzheimer's disease (AD) is the most frequent neurodegenerative condition which causes dementia in elderly people all over the planet [1, 2]. People with AD have two major pathological symptoms including extracellular amyloid plaques and intracellular neurofibrillary tangles (tau protein) [3]. Amyloid beta (Aβ) performs a critical part in AD pathogenesis. Aβ may be found in astrocytes and microglia although it leaves the neurons [4]. Astrocytes are the most abundant glial cells, as well as the scavenging cells in the brain. In addition, they play a significant role in the pathogenesis of AD [5], the functions of which can influence neural survival. Further, they can support neurons in many different ways including energy production of brain, ion, pH balance, synapse formation, remodeling, and oxidative stress regulation [6]. These glial cells participate in clearing Aβ *in vitro* and play a key role in the early stages of AD [7]. Progress in the knowledge of molecular mechanisms of astrocyte may lead to the development of novel therapeutic strategies for neurodegenerative disorders. Aβ-induced synaptic dysfunction reduces tau phosphorylation by activating protein kinase B (AKT), which inhibits glycogen synthase kinase 3 (GSK3β) [8]. Tau is considered as a microtubule-associated protein (MAP), which is expressed in astrocytes and neuritis, which plays a role in regulating microtubule stability [9]. Tau phosphorylation is an early development in AD progression [10]. Aβ1-42 monomers and oligomers alter the phosphorylation of tau protein [8]. The protein kinase C (PKC), as one of the enzymes, is related to amyloid precursor protein (APP) [9, 11]. Regarding the neurons among AD patients, the first abnormality is related to the defect in

PKC signal channels. Inhibiting PKC activity leads to the reduction of learning and memory capacity [12]. The activation of PKC inhibits the activity of GSK3 and hyperphosphorylation of tau in serine 9 [13]. GSK3β inhibition decreases the production of Aβ in the Alzheimer's mouse model, as well as Aβ in the neuronal cell culture [14]. Reactive astrocytes encircling Aβ plaques take part in topical inflammatory responses and modulate calcium signaling [15]. A safe and secure dose of Methamphetamine (METH) probably has a protective effect on neurons and astrocyte cells. Thus, the present study aimed to evaluate the alteration and association between important enzymes such as PKCα, GSK3β, and Cdk5 in the reactive astrocyte induced by Aβ1-42 in the presence of a low dose of METH.

Materials And Methods

All samples used in the study were collected in accordance with the guidelines approved by the ethics committee of our University with approval ID: IR.IAU.DAMGHAN.REC.1398.005.

Preparation of Aβ1–42 peptide

Aβ1–42 peptides were monomerized by dissolution in Hexafluoro-2-propanol (HFIP) (Sigma-920-66-1) for preparation the 1 mM concentration of Aβ, we used 2.2 ml of HFIP They were aliquoted into microcentrifuge tubes. The HFIP was evaporated using a Speed Vac, and the peptide was stored at -20 °C until use. In order to fibril formation, large aggregates of Aβ1-42 were directly dissolved in dH_2O and incubated at 37 ˚C for 72 h [16]. All other chemicals were of analytical reagent grade.

Astrocytes culture and treatment

Primary fetal human astrocytes were isolated from the hypothalamus and cerebral cortex, which were previously isolated from hypothalamus and cerebral cortex of two human fetuses on gestational weeks 9–12 (gift from Bon Yakhteh Laboratory in Tehran) were cultured in DMEM with 10% heat-inactivated fetal bovine serum (FBS) were purchased from Sigma chemical Co., (Sigma-F2442, St. Louis, USA), and kanamycin (50 mg/mL the cells were incubated at 37 °C in %5 CO2, %85 - %95 humidity. 200000-250000 cells were cultured in each well [17]. According to the IC50, after 24 h, METH (donated by Tehran University) and Aβ were added to the well. METH was added to DMEM, containing 10% FBS, to reach the final concentration of 12.5 μM. METH remained in the vicinity of the cell for 24 h. For treatment with Aβ, 10 μM of Aβ was kept at 37 °C for 72 h (fibril formation) and then added to DMEM plus F12 without FBS [18]. Cells were exposed to amyloid for 24 h. All experiments have been performed according to the following procedures: group-1 cells with Aβ, group-2 cells with METH, group-3 cells with METH after 24 h of adding Aβ (Ab + METH, treated group), group-4 cells with Aβ after 24 h of adding METH (METH + Ab, prevention group) and group-5 as control.

MTT assay for estimation of cell viability

Astrocytes were seeded in a 96-well plate (10000, 15000 and 20000 Cells per well), fed with 5% FBS in DMEM, and incubated for 24 hours. Then, they were exposed to 0.8, 1.6, 3.1, 6.2, 12.5, 25, 50, and 100 μM

concentrations of methamphetamine hydrochloride (donated by Tehran University), which were dissolved in water and used for 24-, 48-, and 72-hour treatment. In addition, MTT (Sigma-Aldrich, USA) (5 mg/mL in PBS) was added. We used DMSO to dissolve the crystals. The measured absorbance was at 570 nm.

Cell treatment

Astrocyte cells were cultured in a 6-well plate (200000-250000 cells per well). According to the IC50, METH was added to DMEM containing 10% FBS in order to reach the final concentration of 12.5 mM. Methamphetamine exposure for the cell was performed for 24 h [19]. Regarding the treatment with Aβ, 10 μM of Aβ was kept at 37 ˚C for 72 h (fibril formation), and added to DMEM plus F12 lacking FBS [20] and the cells were exposed to amyloid for 24 h. The related groups included the cells with Aβ (Group 1), METH (Group 2), Ab + METH (METH after adding Aβ for 24 h: Treated group; Group 3), METH + Ab (Aβ after adding METH for 24 h: Prevention group; Group 4), and control.

RNA extraction

Total RNA was isolated from astrocyte culture by using an RNA extraction kit (Roche 11828665001) according to the manufacturer's recommendation. The concentration of RNA samples was determined by measuring optical density at 260 nm. The quality of RNA was confirmed by detecting 18S and 28S bands on agarose gel electrophoresis. The RNA samples were incubated with DNase at room temperature for 15 min in order to remove residual DNA contamination.

cDNA synthesis

The total RNA from each sample was used to generate cDNA with oligo (dT) primers according to the manufacturer's protocol thermo (K1621).

Oligonucleotide primers

GAPDH was used for housekeeping genes, and primer 3 was applied to design all of the primers. Table 1 indicates the primer sequences.

Molecular Analysis

Quantitative real-time PCR analysis

The *GSK3β, Cdk5, PKCa, Bcl-X,* and *Bax* genes related to AD and apoptosis were evaluated by using housekeeping gene (*GAPDH*). The primers were previously checked by conventional RT-PCR and agarose gel (1.5%) electrophoresis. Real-time quantitative polymerase chain reaction (PCR) was performed by using Ampliqon PCR Master Mix (A314406) and Qiagen Rotor-Gene Q system. All of the experiments were performed in triplicates. Table 3 indicates the real-time PCR primers specific for test and *GAPDH* gene. The cycling protocol consisted of an initial 5-min denaturation step at 95 °C, followed by 35 cycles of denaturation at 95°C for 1min, annealing at 60 °C for 1min, extension at 72 °C for 1min and a final 5 min

extension step at 72 °C. CT relative quantification method was used and the obtained CT values were normalized for endogenous reference [21].

Western blotting to prepare total protein extraction

The astrocyte cells were digested in NP40 lysis buffer (CMG-NP40). The cocktail protease and phosphatase inhibitor (Roche 11836153001, 04906845001, respectively) were added to the cell lysate for 30 min at 4 °C. Following centrifugation at 14000 g, the supernatant was stored at -70 ˚C. Then, the protein concentration was determined by using a Bradford Assay Protein Kit (Bio Basic SK3031) according to the manufacturer's protocol [22]. In addition, the proteins were mixed with a loading buffer (TrisHCl 63 mM, glycerol 30%, SDS 2%, Bromophenol blue 0.05%, pH 6.8), and boiled for 5 min at 95 °C. Further, 10% polyacrylamide gel was used. Accordingly, 80 µg of protein was loaded in each well at that time and the electrophoresis was conducted at 125 mV for 1 h. After gel electrophoresis, all proteins were transported into a PVDF membrane with 320 mA for 2 h at 4 °C (Bio-Rad 1620174), and then blocked with BSA 5% for 1.5 h at the room temperature. Membranes were incubated overnight with monoclonal antibody (p-GSK3β-sc-373800) (1:500), monoclonal antibody (GSKα/β- sc-7291) (1:500) at 4 °C, monoclonal (β-Actin (c4) sc-47778) (1:500) at 4 °C and anti-tau (phospho S396 EPR2731) Abcam (1/10000) at 4 °C. Afterwards, the membranes were washed three times for 5 min in Tris-buffer saline solution with 0.1% tween (TBS/T) incubated with 1:10000 diluted anti-mouse antibody (sigma A9044) and 1:2500 diluted goat Anti-rabbit IgG (Elabscience E_AB_1003), respectively. Then, the membranes were washed three times for 5 min in Tris buffer saline solution with 0.1% Tween, and were detected by chemiluminescence. Bands were scanned and the band intensities were calculated by ImageJ. Finally, the bands were normalized to the intensity of β-actin in each sample.

Apoptosis and necrosis survey

Briefly, pre-treated astrocyte cells were harvested with trypsin and washed with 0.01 M PBS twice. Along with centrifugation at 2000 rpm for 5 min, the cells were re-suspended in 500 µl of binding buffer at the density of 1×10^6 cell/ml, along with adding 5 µl Annexin, V-FITC, and 5 µl PI, ((ANXVF-200T)) respectively. Next, the cells were incubated in the dark at 25 °C for 15 min and analyzed by flow cytometry (BD Biosciences, Franklin Lakes, NJ, and USA).

DNA content cell cycle analysis (propidium iodide)

The pre-treated astrocyte cells were harvested with trypsin and washed with PBS by centrifugation at 2000 rpm for 5 min at 4 °C. The cells were re-suspended in cold PBS including DNase-free Ranse (Sigma) and stained with Propidium Iodide (PI) containing 1% Triton X-100 (v/v) (Sigma). The solution was incubated at 20 °C for 30 min (protected from light) and analyzed by flow cytometry (BD Biosciences, Franklin Lakes, NJ, USA) [23].

Hoechst staining assay

The treated astrocyte cells were harvested and washed with PBS. The density of cell should be$1*10^4$ cells/mL in PBS (1:1 v/v). The cells were incubated for 30 min at the room temperature with Hoechst 33342 (Invitrogen, H3570) (5 mg/mL).

Statistical analysis

SPSS v16 and GraphPad Prism were used for statistical analysis. Each of the treatment group was compared with Ab group by using independent sample t-test in real-time PCR. ANOVA followed by Dunnett post hoc test was used to evaluate the results of western blotting analysis. $P < 0.05$ was accepted as the level of significance. All error bars in figures are based on the results of mean ± standard deviation (SD). Each experiment was performed in triplicate.

Results

Effect of methamphetamine on astrocyte viability

The cells were incubated with different concentrations of METH for 24, 48, and 72 hours. The results demonstrated the cellular viability reduction (~ 10%) in the astrocytes within the limited concentrations of METH (0.8, 1.6, 3.1, 6.2, and 12.5 mM) for 24, 48, and 72 hours. Therefore, 12.5 mM concentration of METH was used for further evaluation (data not shown).

Bax and Bcl-x gene expressions

Based on the results, *Bax* expressions in group-3 (Aβ + METH) decreased significantly ($P < 0.05$), while an increase in *Bcl-x* was insignificant compared to group-1 (Aβ) (Fig. 1A-B). The gene expression of *Bax* in group-4 (METH + Aβ) decreased considerably ($P < 0.001$) and *Bcl-x* expression increased ($P < 0.05$) compared to the amount in group-1 (Aβ) (Fig. 1A-B). The ratio of *Bax/Bcl-x* in group-3 (Aβ + METH) decreased about 0.432 fold ($P < 0.05$) compared to group-1 (Aβ), while the ratio of *Bax/Bcl-X* in group-4 (METH + Aβ) decreased about 1.17 fold ($P < 0.05$) compared to the amount in group-1 (Aβ) (Fig. 1C).

GSK3β, Cdk5, and PKCα gene expression

The expression of *GSK3β* and *Cdk5* genes increased ($P < 0.05$) in group-3 (Aβ + METH), while the amount was not significant *in PKCα* compared to the amount in group-1 (Aβ) (Fig. 2A-C). The expressions of *GSk3β*, *Cdk5,* and *PKCα* genes in group-4 (METH + Aβ) decreased ($P < 0.05$, $P < 0.01$ and $P < 0.001$, respectively) compared to the amount in group-1 (Aβ) (Fig. 2D-F).

Gskα, Gskβ, pGsk3βser9, tau-p-ser396 Western blot

The level of GSK3α and GSK3β in group-3 (Aβ + METH) and 4 (METH + Aβ) decreased significantly, compared to that of group-1 (Aβ) (Fig. 3A-B). A significant decrease occurred in GSK3β-ser 9-p expression in group-3 (Aβ + METH) but in group 4 (METH + Aβ) increased compared to the amount in group-1 (Aβ)

(Fig. 3C). P-tau expression in groups 3 and 4 (METH + Aβ) was significant decreased compared to the amount of group-1 (Aβ) (Fig. 3D).

Apoptosis and necrosis analysis by flow cytometry

As shown in Table 2, the percentage of live cells and (early & late) apoptosis increased and decreased, respectively, in all of the treatments compared to the amount in Aβ group. The percentage of early apoptosis decreased in Ab + METH (2.33%) and METH + Ab (2.93%), compared to the amount in Aβ group-1 (Aβ). In addition, 91.5% and 90.3% of live cells occurred in METH + Aβ and Aβ + METH groups compared to the amount in Aβ group (Fig. 4 & Table 2).

Cell cycle arrest in different treatment groups

In Aβ + METH group, astrocytes are exposed to 10 μM Aβ for 24 h, and accordingly with METH for 24 h. Then, astrocyte cells enter S and G2 phase. In METH + Aβ group, they are exposed to METH for 24 h, and accordingly with 10 μM Aβ for 24 h, cells arrest in G2, and enter S compared to the Aβ group. Regarding Aβ + METH group, G1 decreases, enter S phase, and the cells arrest in G2, compared to the Aβ group (Table 3).

Apoptosis detection with Hoechst staining assay

In the Hoechst staining, apoptotic cells (fragmented nuclei) are often observed in Aβ group (Fig. 5).

Discussion

We examined the hypothesis that astrocytes respond to low dose of METH exposure and can effect on tau hyperphosphorilation and apoptosis. So it maybe had a protective effect on AD. The high doses of METH cause dopamine secretion and neurotoxicity. However, moderate activation of dopamine receptors have a protective effect on neurons, also a mild dose of METH increases cell survival by reducing apoptotic cell death [24]. Therefore, we used low dose of METH. The results indicated that a low dose of METH can decrease the amount of apoptosis in the prevention and treatment groups. Also, the effect of a low dose of METH on the expression of PKCα was evaluated. An increase occurred in clearing Aβ while activating the α-secretase plays a role in clearing Aβ and PKCα influence the activity of this enzyme [25]. The results indicated that the effective dose of METH decreases the gene expression of PKCα in the prevention group compared to the experimental model of astrocyte induced with AD, while an increase occurred in the treatment group. Although a highly abundant protein usually has a highly expressed mRNA, some differences may be observed in the amount of protein and mRNA because of the processes between transcription and translation. For example, the difference between protein and mRNA includes the half-life of protein from several minutes to several days, and half-life of mRNA is shorter than 2-7 hours [26]. Thus, it is suggested that the decrease in mRNA expression of PKCa results from its half-life or the presence of miRNA or RNA binding protein which may destroy the pool of mRNA in the cell culture.

In the neuronal damage, Cdk5 and GSK3β are involved in AD leading to tau phosphorylation [27]. In this study, the gene expression of Cdk5 decreased in the prevention group, which increased in the treatment group compared with AD model. The reduction in the amount of Cdk5 in the prevention group indicates that METH can considerably influence Cdk5 expression. A large body of research indicated that Cdk5 is associated with neurotoxicity and neurodegeneration. Other studies reported that METH exposure increases the level of phosphorylated tau, and down-regulation of Cdk5 can prevent from overexpressing phosphorylated tau based on the type of cell line, the concentration of METH, and exposure time (SH-SY5y, 0.5-2 mM, 0-24 h, respectively) [28]. However, the results of the present study indicated that the cell line is astrocyte, exposure time is 24 h, and the concentration of METH is lower since it was designed for treating infected cells.

The stimulation of cells with a protein kinase B (AKT) can inactive the GSK-3 kinases by direct phosphorylation of an inhibitory residue at S21 in GSK-3α or S9 GSK-3β [29]. GSK-3β is the essential kinase that participates in phosphorylation of tau, which could be increase hyperphosphorylation of tau during the intracellular aggregation of Aβ. Furthermore, In AD, activation of GSK-3β- mediated tau phosphorylation reduces its affinity to microtubules and inhibition of GSK-3β effectively reduces tau phosphorylation [30]. In the present study, METH causes to reduce the protein expression of GSK-3α and 3b as their dephosphorylated and activated form compared to Ab group, so the expression of hyperphosphorylated tau protein is decreased in the presence of METH. Also, the protein expression of GSK-3b as their phosphorylated and inactivated form is increased in the presence of METH compared to Ab group, therefore hyperphosphorylation of tau as residue ser396 is decreased in the prevention (METH + Ab) and treatment groups (Ab + METH).

It is worth noting that METH had pretreatment and treatment effect on the astrocytes infected with Aβ since *Bcl-X* increased significantly in both groups. Regarding the *Bcl-X* gene expression, METH and estrogen have a similar effect, both of which increase *Bcl-X* due to the anti-apoptotic effect of the two-mentioned reagents. The results from the previous study show that low concentration of METH without effect on glucose uptake increase the expression of glucose transporter protein-1 (GLUT1) in primary human brain endothelial cell (hBEC) , but a high concentration of METH decrease the glucose uptake and GLUT1 protein level in hBEC culture [31]. Increased GLUT1 can be improving insulin signaling pathway, since AD has been identified as type 3 diabetes [32] increased glycolysis and GLUT1, which are correlated with inactivation of GSK3β or GSK3β-Ser9 phosphorylation that controls the production of ROS [33] In addition, we decided to use low dose of METH because of its effect on the GLUT1 and AD.

During stress conditions, neurons for protection the cells from harmful factors, reactivate their cell cycle and the cell cycle is stopped in the G2 phase [34]. In AD, the neuron cells in areas of the brain are affected by the disease, the G1/S checkpoint often becomes dysregulated, and the prior neurons start the replication of DNA to reach a G2/M phase. Unlike the G1/S checkpoint, the G2/M checkpoint works properly, which prevents from dividing neurons [35]. AD neurons are often arrested in the G2 phase. In the present study, G1, G2, and S were evaluated in all of the treatments. Finally, the cells may go to

autophagy. In other words, the cells remain for a short time in G2 phase, leading to an increase in G1 phase and an increase in G2 in all of the groups except in the treatment group.

Conclusions

In conclusion, since astrocytes as the main supportive cells in CNS and take part in homeostasis, under physiological or pathological conditions, we used low dose of METH on reactive astrocyte and evaluated the main signaling pathway in AD. Low-dose of METH reduced Early & late apoptosis and increased live cell. It also increased and decreased *Bax* and *Bcl-X* gene expression, respectively and also decreased the gene and protein expression of *GSK* as a marker of AD. The findings indicated the beneficial use of a low dose of METH in managing AD. Thus, it is suggested that the used dose can be considered as a new potential therapeutic method.

Declarations

Acknowledgement

This study was supported by grant from University of Tehran of Iran.

Funding

This research did not receive any specific grant from funding agencies in the public, commercial, or nonprofit sectors.

Conflict of interest

The authors declare that they have no conflict of interest.

Ethical approval

All samples used in the study were collected in accordance with the guidelines approved by the ethics committee of our University with approval ID: IR.IAU.DAMGHAN.REC.1398.005.

Authors' contributions

Investigation: Bita Soltanian; Conducted the experiments and Writing-review & editing: Bita Soltanian and Marzieh Dehghan Shasaltaneh; Data analysis: Bita Soltanian, Marzieh Dehghan Shasaltaneh and Gholam Hossein Riazi; Supervision: Marzieh Dehghan Shasaltaneh, Nahid Masoudiyan and Gholam Hossein Riazi; and All authors have read and approved the manuscript before submission.

References

1. Hardy. J, DJ. Selkoe (2002) The amyloid hypothesis of Alzheimer's disease: progress and problems on the road to therapeutics. sci 297(5580): 353-356.

2. Wu. X.-L et al (2017) Tau-mediated neurodegeneration and potential implications in diagnosis and treatment of Alzheimer's disease. Chinese Med J 130(24): 2978-2990.
3. Iqbal. K, F. Liu, C.-X (2016) Gong, Tau and neurodegenerative disease: the story so far. Nat Rev Neurol 12(1): 15-27.
4. Selkoe. DJ (2001) Alzheimer's disease: genes, proteins, and therapy. Physiol Rev 81(2): 741-766.
5. Batarseh. YS et al., (2016) Amyloid-β and astrocytes interplay in amyloid-β related disorders. International journal of molecular sciences 17(3): 338-357.
6. Valles. SL (2012) Astrocytes and the important role in the future research of brain. J Alzheimers Dis Parkinsonism 2: e127-e128.
7. Fakhoury. M (2018) Microglia and astrocytes in Alzheimer's disease: Implications for therapy. Curr Neuropharmacol 16(5): 508-518.
8. Garwood. C et al (2011) Astrocytes are important mediators of A β-induced neurotoxicity and tau phosphorylation in primary culture. Cell Death Dis 2(6): e167-e167.
9. Tan. MG et al (2010) Genome wide profiling of altered gene expression in the neocortex of Alzheimer's disease. J Neurosci RES 88(6): 1157-1169.
10. Bierer. LM et al (1995) Neocortical neurofibrillary tangles correlate with dementia severity in Alzheimer's disease. Arch Neurol-Chicago 52(1): 81-88.
11. Hooper. C, Killick. R, Lovestone. S (2008) The GSK3 hypothesis of Alzheimer’s disease. J Neurochem 104(6): 1433-1439.
12. Sun. M-K, Alkon. DL (2014) The “memory kinases”: Roles of PKC isoforms in signal processing and memory formation, in Progress in molecular biology and translational science. Els 31-59.
13. Isagawa. T et al (2000) Dual effects of PKNα and protein kinase C on phosphorylation of tau protein by glycogen synthase kinase-3β. Biochem Bioph Res Co 273(1): 209-212.
14. Samadi. A et al (2011) Cholinergic and neuroprotective drugs for the treatment of Alzheimer and neuronal vascular diseases. II. Synthesis, biological assessment, and molecular modelling of new tacrine analogues from highly substituted 2-aminopyridine-3-carbonitriles. Bioorgan Med Chem 19(1): 122-133.
15. Rodriguez. J et al (2009) Astroglia in dementia and Alzheimer's disease. Cell Death Differ 16(3): 378-385.
16. Azzopardi. M, Farrugia. G, Balzan. R (2017) Cell-cycle involvement in autophagy and apoptosis in yeast. Mech Ageing Dev 161: 211-224.
17. Sharif. A, Prevot. V (2012) Isolation and culture of human astrocytesSeries. In: Astrocytes. Springer 137-151
18. White. J. A, Manelli. A. M, Holmberg. K. H, Van. Eldik. L. J, LaDu. M. J (2005) Differential effects of oligomeric and fibrillar amyloid-β1–42 on astrocyte-mediated inflammation. Neurobiology of disease 18(3): 459-465.

19. Qiu. C et al (2016) Exendin-4 protects Aβ (1-42) oligomer-induced PC12 cell apoptosis. Am J Transl Res 8(8): 3540-3548.
20. White. JA et al (2005) Differential effects of oligomeric and fibrillar amyloid-β1–42 on astrocyte-mediated inflammation. Neurobiol Dis 18(3): 459-465.
21. Schmittgen. TD, Livak. KJ (2008) Analyzing real-time PCR data by the comparative C T method. Nat Protoc 3(6): 1101-1108.
22. Hammond. JB, Kruger. NJ (1988) The bradford method for protein quantitation, in New Protein Techniques. Springer 25-32.
23. Riccardi. C, Nicoletti. I (2006) Analysis of apoptosis by propidium iodide staining and flow cytometry. Nat Protoc 1(3): 1458-1461.
24. Rau. TF et al (2011) Low dose methamphetamine mediates neuroprotection through a PI3K-AKT pathway. Neuropharmacology 61(4): 677-686.
25. Kim. T, Hinton. DJ, Choi. D-S (2011) Protein kinase C-regulated Aβ production and clearance. Int J Alzheimer Dis 2011: 1-8.
26. Vogel. C, Marcotte. EM (2012) Insights into the regulation of protein abundance from proteomic and transcriptomic analyses. Nat Rev Genet 13(4): 227-232.
27. Castro-Alvarez. JF et al (2014) Long-and short-term CDK5 knockdown prevents spatial memory dysfunction and tau pathology of triple transgenic Alzheimer's mice. Front Aging Neurosci 6: 243-253.
28. Xiao. N et al (2018) CDK5-mediated tau accumulation triggers methamphetamine-induced neuronal apoptosis via endoplasmic reticulum-associated degradation pathway. Toxicol Lett 292: 97-107.
29. Ding. L, Billadeau. DD (2020) Glycogen synthase kinase-3β: a novel therapeutic target for pancreatic cancer. Expert Opin Ther Tar 24(5): 417-426.
30. Avila. J et al (2012) Tau phosphorylation by GSK3 in different conditions. Int J Alzheimer Dis 2012: 1-8.
31. Muneer. PA et al (2011) Impairment of brain endothelial glucose transporter by methamphetamine causes blood-brain barrier dysfunction. Mol Neurodegener 6(1): 23-36.
32. Ghahghaei. A et al (2013) The protective effect of crocin on the amyloid fibril formation of Aβ42 peptide in vitro. Cell Mol Biol Lett 18(3): 328-39.
33. Nguyen. HM et al (2016) Reduction in cardiolipin decreases mitochondrial spare respiratory capacity and increases glucose transport into and across human brain cerebral microvascular endothelial cells. J Neurochem 139(1): 68-80.
34. Bonda. DJ et al (2010) Pathological implications of cell cycle re-entry in Alzheimer disease. Expert Rev Mol Med 12: 1-11.
35. Wojsiat. J et al (2015) Oxidative stress and aberrant cell cycle in Alzheimer's disease lymphocytes: diagnostic prospects. J Alzheimer Dis 46(2): 329-350.

Tables

Table 1 Primers used for Real-time PCR

Primer	Forward	Revers	length
GAPDH	GACCACTTTGTCAAGCTCATTTCC	GTGAGGGTCTCTCTCTTCCTCTTG	168bp
Bax	TGGAGCTGCAGAGGATGATTG	GAAGTTGCCGTCAGAAAACATG	98bp
Bcl-x	CTGAATCGGAGATGGAGACC	TGGGATGTCAGGTCACTGAA	211bp
Pkcα	GGTCCACAAGAGGTGCCATG	AAGGTGGGGCTTCCGTAAGTG	122bp
Gsk3β	ACAACAGTGGTGGCAACTCC	TTCTTGATGGCGACCAGTTCT	89bp
CDK5	GGAAGGCACCTACGGAACTG	CGGCACACCCTCATCATCATCG	102bp

Table 2 Apoptosis and necrosis analysis by flow cytometry

The percentage of cells					
Group	Aβ	METH	Aβ+METH	METH+Aβ	Control
Live cell	89	92.4	90.3	91.5	95.3
Late apoptosis	2.02	2.06	2.47	2.45	1.22
Early apoptosis	4.13	3.91	2.33	2.93	1.05
Early & late apoptosis	6.15	5.97	4.8	5.38	2.27
necrosis	4.87	1.62	4.95	3.13	2.45

Table 3 Cell cycle arrest in different treated groups

Group	G1	S	G2
Aβ	64.45%	19.35%	14.35%
METH	63.92	21.71%	11.8%
Aβ + METH	44.07%	29.76%	22.64%
METH + Aβ	66.44%	13.43%	13.05%
Control	70.54%	15.57%	8.02%

Figures

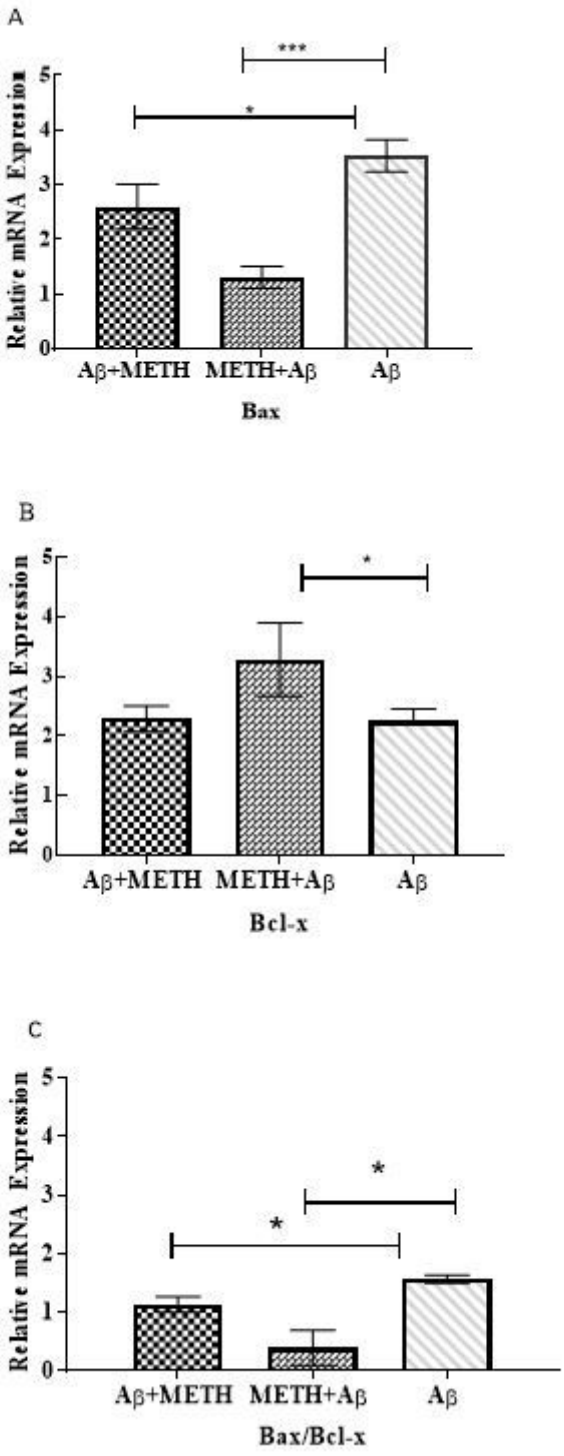

Figure 1

The effect of METH on the expression of Bax and Bcl-X genes. The values put onto each graph represent the relative fold change calculated by calibrating the ΔCt data Bax and Bcl-X gene expressions in several experiments. (A) Bax decreases in group-3 (Aβ + METH) and group-4 (METH + Aβ) in compare to group1 (Aβ) (P = 0.035 and P = 0, respectively). (B) An increase in Bcl-X is not significant in group-3 (Aβ + METH), and group-4 (METH + Aβ) increases (P = 0.056). (C) The ratio of Bax/Bclx in group-3 (Aβ + METH) and group-4 (METH + Aβ) was decreases in compare to group1 (Aβ) (P = 0.035). Error bars indicate SD. The level of significance was considered as * P ≤ 0.05. group-1 (Aβ), group-2 (METH), group-3 (Aβ + METH), group-4 (METH + Aβ).

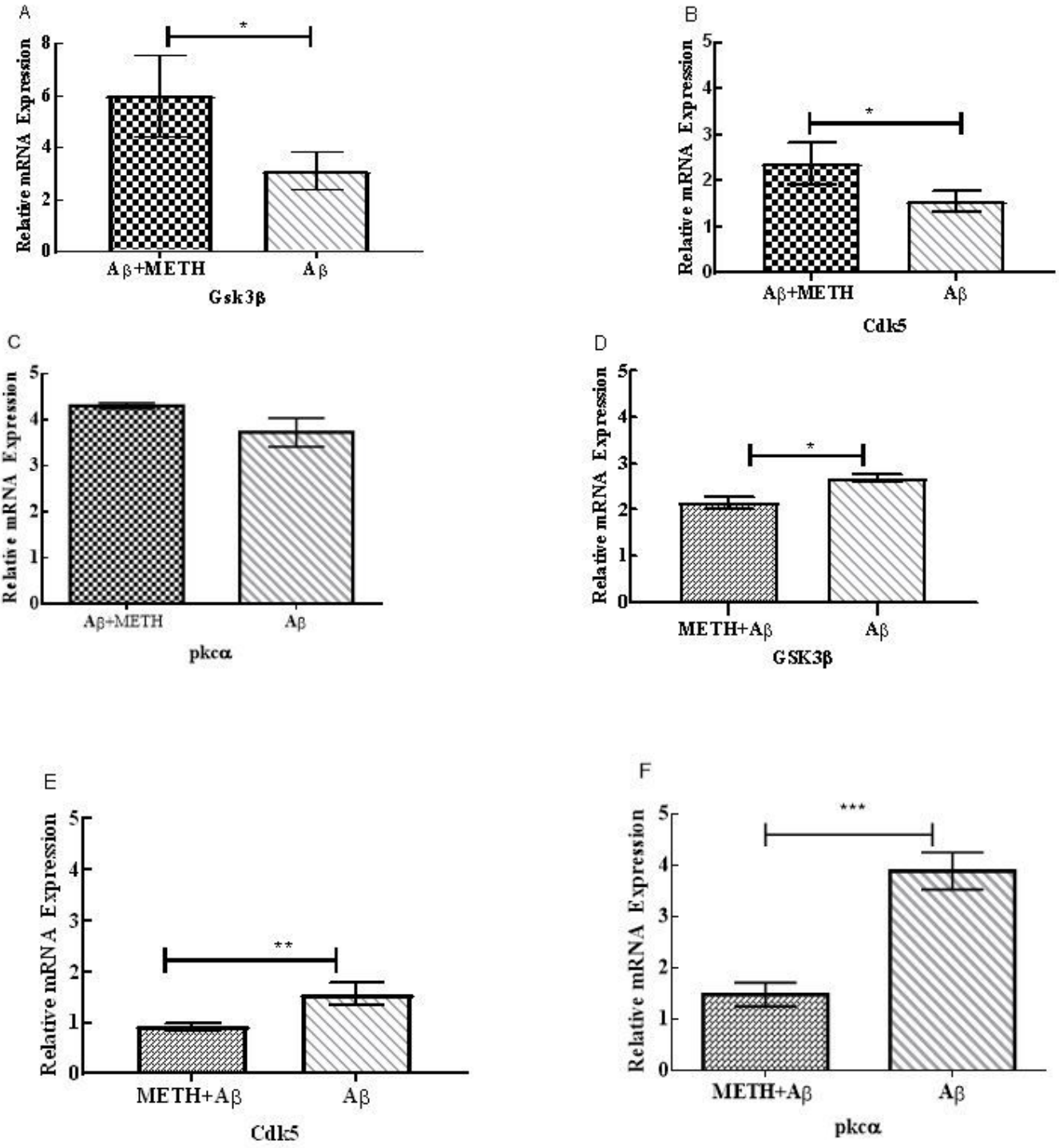

Figure 2

The effect of METH on the expression of GSK3β, Cdk5 and PKCα genes. The values put onto each graph represent the relative fold change, calculated by calibrating the ΔCt data for GSK3β, Cdk5, and PKCα gene expressions in several experiments. (A & B) GSK3β and Cdk5 in group-3 (Aβ + METH) increased (P = 0.043 and P = 0.015, respectively), but (D, E, F) GSK3β, PKCα and Cdk5 in group-4 (METH + Aβ) decreased (P = 0.045, P = 0.01 and P = 0.001, respectively). The increase in PKCα in group-3 (Aβ + METH) is not significant compared to group-1 (Aβ). Error bars indicate SD. The level of significance was considered as * $P \leq 0.05$. group-1 (Aβ), group-2 (METH), group-3 (Aβ + METH), group-4 (METH + Aβ).

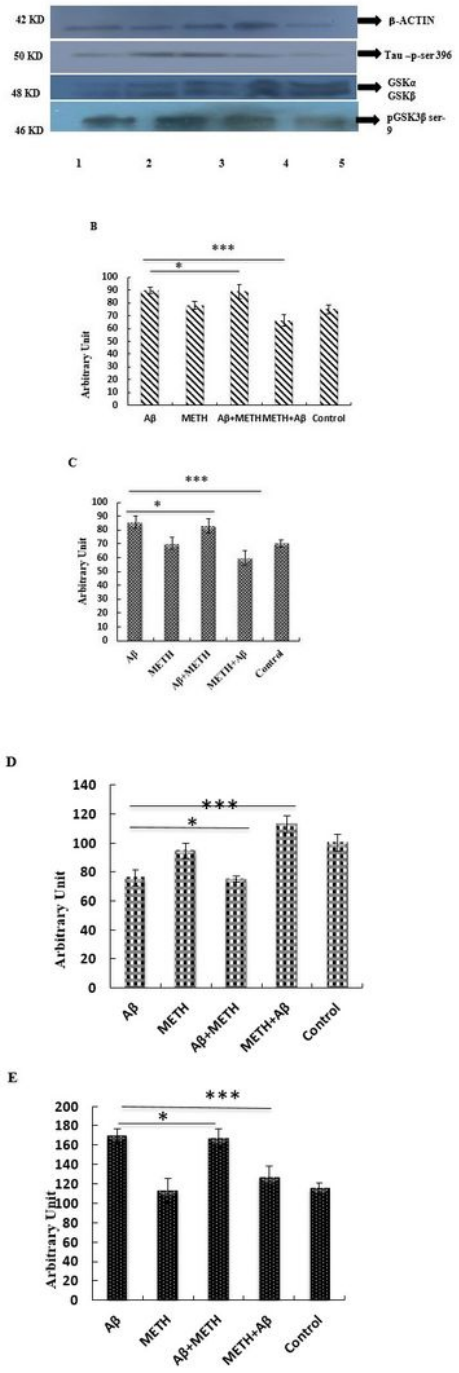

Figure 3

The effect of METH on the expression of (B) GSK3α, (C) GSK3β, (D) p-GSK3β-ser9 and (E) p-tau-ser396. All of them decreased in group-3 (Aβ + METH) but GSK3α, GSK3β, and p-tau-ser396 decreased in group-4 (METH + Aβ) compared to group-1 (Aβ), while p-GSK3β-ser9 increased in group-4 (METH + Aβ) compared to group-1. The numbers below the western blot including the following groups: 1 (Aβ), 2 (METH), 3 (Aβ + METH), 4 (METH + Aβ), 5 (control).

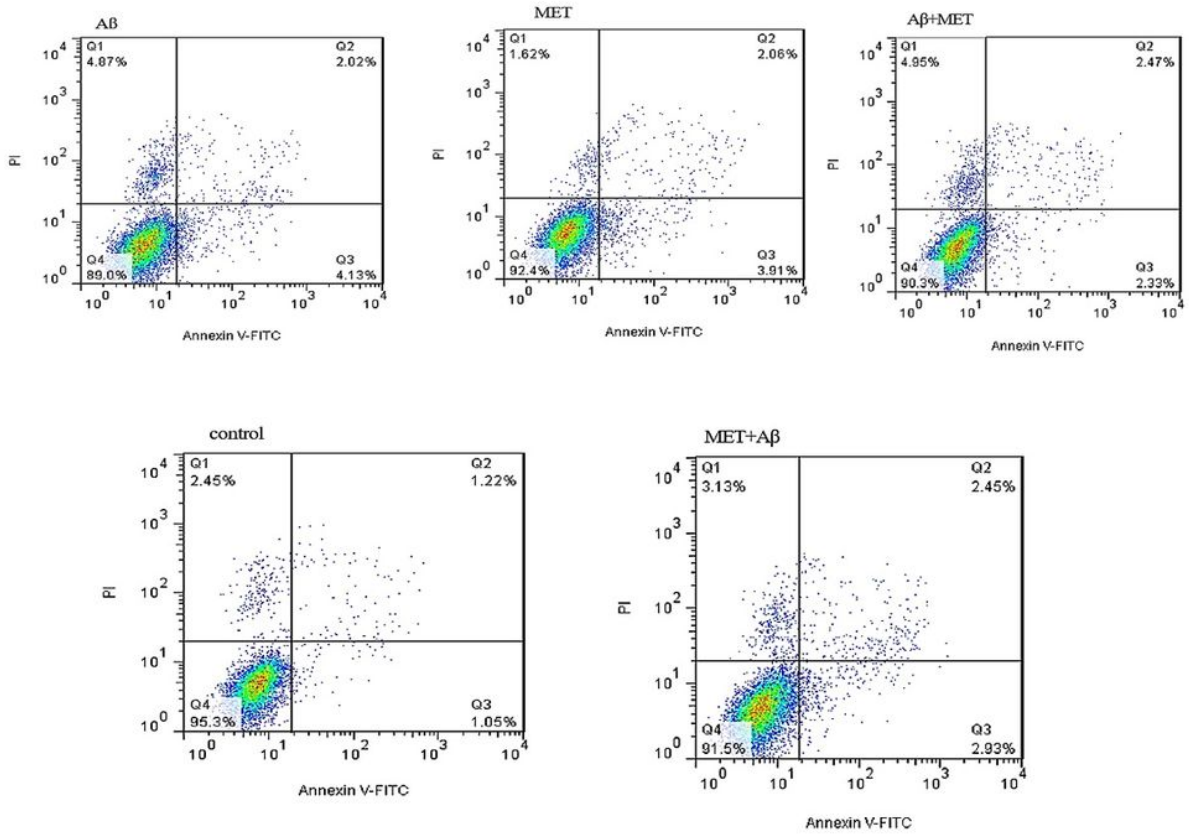

Figure 4

The effect of METH on the apoptosis in astrocyte cell. the control group shows the untreated astrocyte cells after 72 h, (Aβ) group treated with 10 μM Aβ for 24 h, (METH) group after astrocyte was treated with 12.5 μM METH for 24 h, (Aβ + METH) group with flow cytometry carried out on astrocyte which was treated for 24 h with Aβ and then 24 h with METH, (METH + Aβ) group that astrocyte was treated with METH for 24 h and after that treated with Aβ for 24 h, and then flow cytometry was analyzed in both treated and untreated group. Q1: PI= positive, Annexin V FITC negative (necrosis), Q2: PI= positive, Annexin V FITC positive (late apoptosis), Q3 PI= negative, Annexin V FITC positive (early apoptosis), Q4: PI= negative, Annexin V FITC negative (live cell).

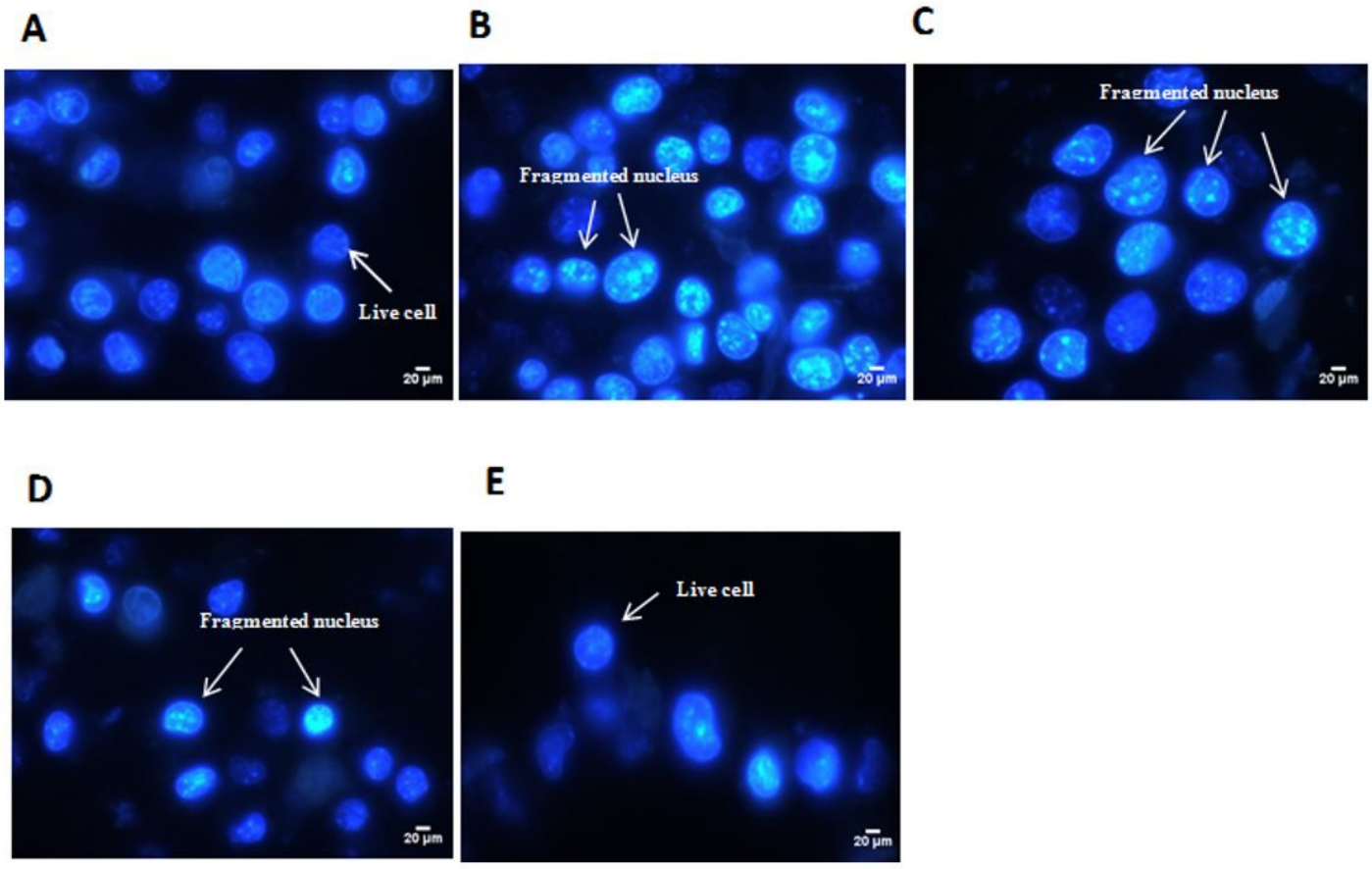

Figure 5

Photomicrograph of apoptotic changes in astrocytes treated with 10 µM Aβ and 12.5 µM METH for 24 h using Hoechst assay visualized by fluorescence microscopy and photographed, Scale bar 20 µm. (A) Control, (B) Aβ, (C) Aβ + METH, (D) METH + Aβ (E) METH.